Resonantly inverted microwave transmissivity threshold of metal grids

2010 New J. Phys. 12 063007

(http://iopscience.iop.org/1367-2630/12/6/063007)

New Journal of Physics
The open-access journal for physics

Resonantly inverted microwave transmissivity threshold of metal grids

J D Edmunds[1,3], A P Hibbins[1], J R Sambles[1] and I J Youngs[2]
[1] Electromagnetic Materials Group, School of Physics, University of Exeter, Stocker Road, Exeter EX4 4QL, UK
[2] Dstl, Salisbury SP4 0JQ, UK
E-mail: j.d.edmunds@ex.ac.uk

New Journal of Physics **12** (2010) 063007 (7pp)
Received 2 February 2010
Published 4 June 2010
Online at http://www.njp.org/
doi:10.1088/1367-2630/12/6/063007

Abstract. The microwave transmission of arrays of square patches, each rotated by 45° from the axes of the square lattice on which they are positioned, has been experimentally studied as a function of metal occupancy. At low frequencies, the microwave transmissivity drops on passing through the connectivity threshold (50 per cent occupancy), as one would expect. However, quite counter-intuitively, near the onset of diffraction, resonant phenomena induce a complete reversal in the sense of this transmissivity switch, i.e. the transmission is seen to increase as the metal occupancy is increased.

Contents

1. Introduction

In recent years there has been substantial interest in the electromagnetic properties of patterned metal surfaces and thin films. Much of this work [1]–[3] has focused on the transmissive properties of films in the visible region, but there is also a long history of radar-related research [4]–[7].

[3] Author to whom any correspondence should be addressed.

Ebbesen and co-workers' observation of enhanced optical transmission (EOT) [1] through sub-wavelength hole arrays in noble metal films in the visible regime reignited considerable interest in the field. They demonstrated that such transmission could exceed that predicted by Bethe's theory [8] for a single aperture by many orders of magnitude. This EOT phenomenon is commonly attributed to the excitation of coupled surface plasmons on each side of the hole array [9,10]. At microwave frequencies, where metals behave as near-perfect conductors, there is a substantial body of work that has explored hole arrays (inductive meshes) and their complementary structures, i.e. patch arrays (capacitive meshes) (see [11] and references therein). These structures are commonly referred to as frequency selective surfaces (FSSs) due to their behaviour in the long-wavelength limit. However, resonant behaviour can be observed [12]–[14], either as a transmission peak for hole arrays or as a reflection peak for patch arrays, when the incident wavelength, λ_0, is close to the grating pitch, λ_g. They have been successfully modelled using equivalent circuit theories [12,15,16] where capacitive and inductive elements determine the resonant frequency of the array and resistive components determine the loss. The resonances observed in these structures are essentially identical to those associated with EOT in the visible regime since they both result from diffraction phenomena associated with the periodicity of the array. García de Abajo *et al* [17] have provided further discussion of this resonant behaviour in their study of periodically perforated layers of perfect electrical conductors (PECs), illustrating that complete transmission is possible near the onset of diffraction, regardless of hole size. This resonant mode observed was described as a structural resonance dependent on the periodicity of the structure, being due to the accumulation of long-distance in-phase coherent multiple scattering from the holes. Their results have been experimentally verified in thick ($\sim$1 mm) hole arrays by Hou *et al* [18].

The patches and holes in many previous studies [12]–[14] have been aligned so that their sides lie parallel to those of the unit cell. However, in this study (and a small number of others [19, 20]), the square patches (holes) are rotated by 45° compared to this conventional geometry, giving connectivity between neighbouring patches at a 50% metal occupancy (figure 1(b)). This allows the dependence of the microwave transmission on the metal occupancy either side of the connectivity threshold (when the metal patches switch from disconnected to connected) to be fully explored. A regular orientation with the patches aligned parallel to the periodicity direction would not allow this study since metallic connectivity within the structure would not be present until 100% metal occupancy had been reached. Conventional wisdom would have it that the high microwave transmissivity of a regular array of patches will switch off on increase of the metal occupancy through the connectivity threshold (or for a somewhat more random array at a 'percolation threshold') [7]. However, the remarkable result presented here is that, for frequencies close to the diffraction edge, the existence of the resonance previously discussed causes the microwave transmittance to go from zero to unity through this threshold—a complete reversal of the expected behaviour at lower frequencies. Counter-intuitive phenomena such as reduced transmission through ultrathin metallic hole arrays compared to that of transmission through thick hole arrays has been reported at optical frequencies by Braun *et al* [21].

In this study, we investigate the resonances close to the diffraction edge for both connected and disconnected structures and explore fully this anomalous behaviour in the microwave transmissivity close to the connectivity threshold.

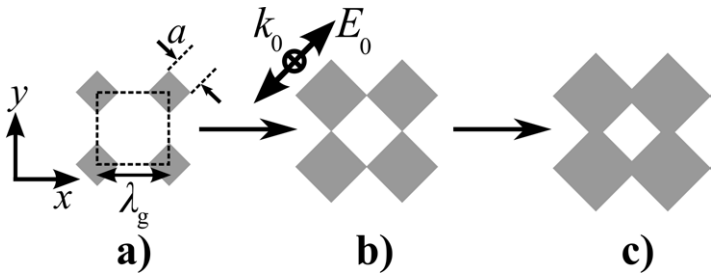

Figure 1. Schematic illustrating the increase of patch size with fixed pitch to form a fully connected conducting network. (Grey represents aluminium and the dotted line indicates the unit cell of the array.) Orientation of the incident electric vector is illustrated.

2. Results and discussion

Samples were produced using a square array geometry of pitch $\lambda_g = 7.02$ mm with a square patch of side length a on each lattice point (figure 1).

Each square patch is orientated with its sides at 45° to the primary lattice vectors. The samples are formed by employing traditional photolithographic and chemical etching techniques to pattern a nominally 60 nm thick aluminium layer on a 75 μm Mylar® substrate. Note that while the thickness of the aluminium layer is much less than the skin depth at the frequency range studied ($\sim$1 μm), it is essentially completely opaque to microwaves due to its Drude-like dielectric function $\mathrm{Im}(\varepsilon) \to \infty$ manifested as a large impedance mismatch. A series of samples were fabricated with metal occupancy $0 \leqslant X \leqslant 100\%$ (no metal to continuous aluminium) by variation of the patch side length a (figure 1) while maintaining the pitch λ_g. Any sample with $a > 4.965$ mm ($X > 50\%$) results in overlapping patches to form a conducting mesh network (hole array).

A collimated microwave beam is incident normal to a sample, which is supported on a 3 mm thick sheet of expanded polystyrene (refractive index $\sim$1 at these frequencies) and placed behind a 100 mm $\times$ 100 mm aperture formed from microwave absorbing material. Transmission measurements in the frequency range $12.4 \leqslant \nu \leqslant 60$ GHz are performed, and normalized to transmission through the aperture and polystyrene sheet without a sample. Typical results are shown in figure 2. First-order diffraction occurs at 42.7 GHz due to the 7.02 mm periodicity.

Modelled responses are obtained with a finite element method (FEM) model[4], using the unit cell illustrated in figure 1(a), together with periodic boundary conditions. We assume that the sample is infinite in extent in the xy-plane and that a perfect plane wave is incident. In reality, of course, both the sample and beam spot are finite. There is also a small incident angle spread of $\sim$1–2° inherent in the experimental technique, and this accounts for the small discrepancy between the data and the model near the diffraction edge where a double peak is observed in the data. This arises from a band gap close to the diffraction edge and the consequential existence of a mode associated with each band edge. At normal incidence, field symmetry prevents coupling to the upper frequency mode. However, at other angles of incidence the symmetry is broken and the wave can couple to both the upper and the lower branch. Then, because of the finite angle

[4] Finite element modelling: HFSS™, Ansoft Corporation, Pittsburgh CA, USA.

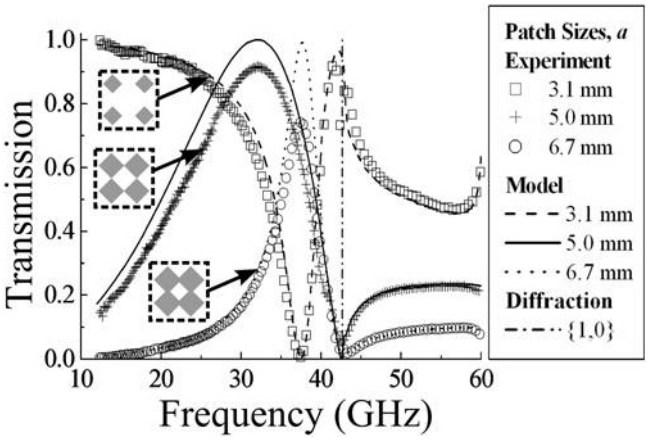

Figure 2. Transmission measurements for three patch sizes on a square array of pitch 7.02 mm. Normal incidence, electric-field vector polarized parallel to patch side. Schematic diagrams illustrate the connectivity of the structure.

spread in the incident beam, this higher frequency mode is seen for normal incidence resulting in a double-peak feature in transmission. Further, the thin metal patches have been represented as two-dimensional (i.e. zero-thickness) objects and defined as PECs in the model. While this is generally a good approximation for the microwave regime, it does lead to other discrepancies between the model and data due to loss within the thin metal layer. This is apparent in the data for the 5.0 and 6.7 mm patch side samples close to the resonant peak. Better agreement between model and data can be achieved by introducing finite thickness and loss within the metal, but such modelling is computationally inhibiting. Metals in the microwave regime have very large refractive indices ($\sim 10^3$) and the thickness of our film is very sub-wavelength ($\sim \lambda/10^5$). Then to maintain sensible aspect ratios of the finite element model tetrahedra, a very dense mesh in the metal relative to that in the incident medium is therefore required to accurately describe the fields. In addition, the mesh in the incident medium has to be graded in density in order to match with the mesh in the metal at the metal–air interface. This requires a large amount of computer memory and many hours of computing time to solve the fields within these elements. Therefore, the simple two-dimensional PEC approximation has been employed throughout the remainder of this study.

At low frequencies the disconnected arrays of patches ($a < 4.965$ mm) exhibit low-pass frequency filtering behaviour commonly seen for a regular capacitive patch array [11]. This is simply because long wavelengths cannot drive currents around the system. The connected arrays ($a < 4.965$ mm) exhibit high-pass frequency filtering behaviour associated with inductive meshes [11] since currents are able to propagate in the continuous network of metal. Samples of a given metal occupancy ($X\%$) are the inverse of those with an occupancy of $(100 - X)\%$. Thus, using Babinet's principle [22] and assuming a zero-thickness perfect conductor, samples with $X\%$ occupancy will have a normal incidence transmissivity T_X, while $(100 - X)\%$ samples have a transmissivity of $1 - T_X$.

Each of the samples exhibits a resonance near the diffraction edge that can be seen as a *minimum* in transmission for the disconnected samples and a *maximum* in transmission for the connected patch samples. These resonances are similar to those reported by García de Abajo *et al* [17], being of geometrical nature, associated with the periodicity of the array, and are

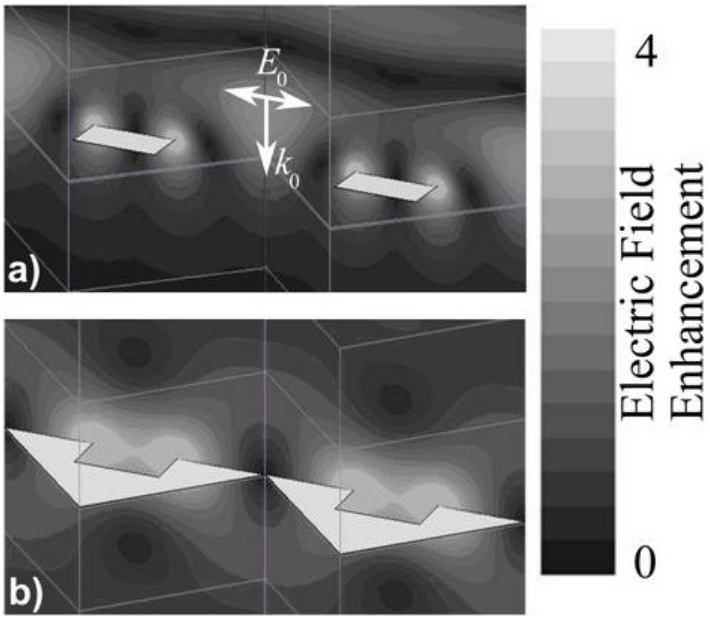

Figure 3. Electric field plots from FEM modelling of two neighbouring unit cells, plotted through the middle of the unit cell in the E_0–k_0 plane for the (a) $a = 3.1$ mm and (b) $a = 6.7$ mm samples on resonance. Light grey shading indicates electric field enhancement of four times and black shading indicates zero electric field enhancement. White indicates PEC regions.

hybridized with the dipolar mode of each patch/hole. Indeed, one may examine the modelled fields to more fully understand their origin (figure 3).

For the disconnected patch array (figure 3(a)), there exists a standing wave across the patch edge along the direction of polarization with the fields showing dipolar character. The complementary structure (figure 3(b)) also shows dipolar behaviour in its field profile with large fields in the hole. Near-field interaction between neighbouring patches and holes can be seen on the field plots. Since the patches are disconnected, the linkages between unit cells are supported by displacement currents, whereas the connected array can support propagating currents. The strength of the evanescent diffracted orders is greatest closest to the onset of the first propagating diffracted order and it is these evanescent fields that lead to the resonant interaction between neighbouring patches/holes. There are two transmission channels present, a resonant and a non-resonant contribution, and it is the interference between these two channels that leads to the characteristic Fano-resonance [23] shape. As discussed in [24], we see that the diffraction due to scattering from small patches/holes induces narrow resonances close to the diffraction edge, while the diffraction from larger patches/holes induces a broadening of the resonance and a shift to lower frequencies.

The transmission as a function of metal occupancy at a series of fixed frequencies is plotted in figure 4.

At dc the transition from full transmission to zero transmission would be expected to take the form of a perfect step function at 50% occupancy with an infinite negative gradient. However, for a finite frequency the transition takes a different form. At 12.4 GHz the transition still exhibits an edge, but it is less sharp because the incident wavelength is now closer to the

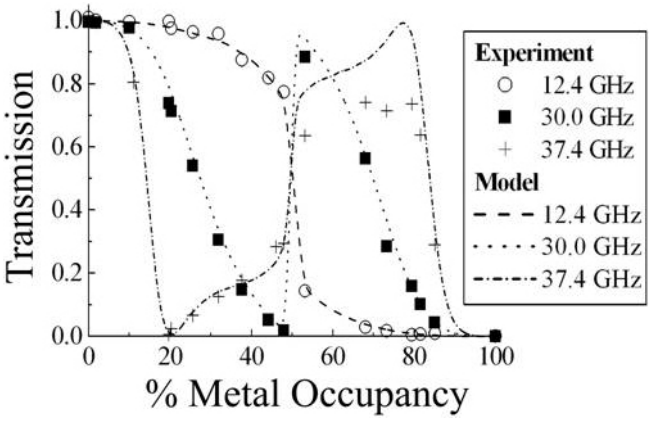

Figure 4. Normal incidence transmission measurements as a function of metal occupancy for a square array of square patches orientated at 45° with respect to the unit cell. The model is for PEC metal.

grating pitch λ_g and the perturbation due to the resonance is becoming increasingly important. This results in a smoothing of the dependence on metal occupancy as we pass through the connectivity point.

At frequencies closer to the onset of diffraction, the perturbation due to the resonance results in a strikingly different transition profile. Transmission for 30.0 GHz shows that the effect is sufficiently strong such that the transmission behaviour on passing through 50% occupancy is of opposite sign. The transmission no longer continually decreases across the whole of the metal occupancy range since the structure is strongly resonant close to the connectivity threshold. At 37.4 GHz the transition profile is further perturbed. Approximate 180° rotation symmetry of the transmission spectrum is visible about the 50% occupancy condition, $T = 0.5$ point, due to Babinet's principle [22]. However, it is apparent that while the resonant transmission is reduced to $T = 0$ at about 20% metal occupancy, the maximum at 80% occupancy reaches only $T = 0.8$. This, as previously discussed, is due to the dissipation in the metal, which on resonance may be substantial and is not accounted for in the PEC model.

3. Conclusions

In summary, a transmission study through a series of square patch/hole arrays with various connectivity and metal occupancies has been presented. It has been found that the variation of transmission with metal occupancy does not always take the form of a step function as anticipated, but is heavily frequency dependent. This frequency dependence is due to the periodicity of the array and associated resonances. The elements that comprise the arrays are able to interact by means of evanescent diffracted orders in the near field to give resonant transmission/reflection causing strong perturbation to the metal occupancy-dependent transmission. Most strikingly, at frequencies close to the diffraction edge the expected decrease in transmission on crossing the 50% occupancy (connectivity) threshold is completely reversed. This effect of the combination of a resonance with a connectivity threshold leading to reversed behaviour will of course extend to somewhat disordered systems and percolation structures.

Acknowledgments

JDE is grateful to Dstl and EPSRC for financial support through the ICASE scheme, and APH wishes to acknowledge the continued support of the EPSRC through his Advanced Research Fellowship.

References

[1] Ebbessen T W, Lezec H J, Ghaemi H F, Thio T and Wolff P A 1998 *Nature* **391** 667
[2] Martín-Moreno L, García-Vidal F J, Lezec H J, Pellerin K M, Thio T, Pendry J B and Ebbesen T W 2001 *Phys. Rev. Lett.* **86** 1114
[3] Genet C and Ebbesen T W 2007 *Nature* **445** 39
[4] Antonets I V, Kotov L N, Nekipelov S V and Karpushov E N 2004 *Tech. Phys.* **49** 1496
[5] Kelly R J, Lockyear M J, Suckling J R, Sambles J R and Lawrence C R 2007 *Appl. Phys. Lett.* **90** 223506
[6] Hansen R C and Pawlewicz W T 1982 *IEEE Trans. Microw. Theory Tech.* **30** 2064
[7] Lagarkov A N, Rozanov K N, Sarychev A K and Simonov N A 1997 *Physica* A **241** 199
[8] Bethe H A 1944 *Phys. Rev.* **66** 163
[9] Ghaemi H F, Thio T, Grupp D E, Ebbesen T W and Lezec H J 1998 *Phys. Rev.* B **58** 6779
[10] Popov E, Neviere M, Enoch S and Reinisch R 2000 *Phys. Rev.* B **62** 16100
[11] Munk B A 2000 *Frequency Selective Surfaces: Theory and Design* (New York: Wiley)
[12] Ulrich R 1967 *Infrared Phys.* **7** 37
[13] Shanahan S T and Heckenberg N R 1981 *Appl. Opt.* **20** 4019
[14] Ulrich R 1968 *Appl. Opt.* **7** 1987
[15] Whitbourn L B and Compton R C 1985 *Appl. Opt.* **24** 217
[16] Dawes D H, McPhedran M C and Whitbourn L B 1989 *Appl. Opt.* **28** 3498
[17] García de Abajo F J, Gómez-Medina R and Sáenz J J 2005 *Phys. Rev.* E **72** 016608
[18] Hou B, Hang Z H, Wen W J, Chan C T and Sheng P 2006 *Appl. Phys. Lett.* **89** 131917
[19] Compton R C and Rutledge D B 1985 *IEEE Trans. Microw. Theory Technol.* **33** 1083
[20] Compton R C, Macfarlane J C, Whitbourn L B, Blanco M M and McPhedran R C 1984 *Opt. Acta* **31** 515
[21] Braun J, Gompf B, Kobiela G and Dressel M 2009 *Phys. Rev. Lett.* **103** 203901
[22] Babinet M 1837 *C. R. Acad. Sci.* **4** 638
[23] Fano U 1961 *Phys. Rev.* **124** 1866
[24] Bravo-Abad J, Martín-Moreno L, García-Vidal F J, Hendry E and Rivas J G 2007 *Phys. Rev.* B **76** 241102